In situ attenuated total reflection infrared (ATR-IR) study of the adsorption of NO2-, NH2OH, and NH4+ on Pd/Al2O3 and Pt/Al2O3

3 AUTHORS:

Sune Dalgaard Ebbesen
Innovation Fund Denmark
65 PUBLICATIONS **1,438** CITATIONS

SEE PROFILE

Barbara L Mojet
University of Twente
80 PUBLICATIONS **1,803** CITATIONS

SEE PROFILE

Leon Lefferts
University of Twente
196 PUBLICATIONS **3,603** CITATIONS

SEE PROFILE

In Situ Attenuated Total Reflection Infrared (ATR-IR) Study of the Adsorption of NO_2^-, NH_2OH, and NH_4^+ on Pd/Al_2O_3 and Pt/Al_2O_3

Sune D. Ebbesen,[†] Barbara L. Mojet, and Leon Lefferts*

Catalytic Processes and Materials, Faculty of Science and Technology, Institute of Mechanics Processes and Control Twente (IMPACT) and MESA+ Institute for Nanotechnology, University of Twente, P.O. Box 217, 7500 AE, Enschede, The Netherlands

In relation to the heterogeneous hydrogenation of nitrite, adsorption of NO_2^-, NH_4^+, and NH_2OH from the aqueous phase was examined on Pt/Al_2O_3, Pd/Al_2O_3, and Al_2O_3. None of the investigated inorganic nitrogen compounds adsorb on alumina at conditions presented in this study. $NO_2^-{}_{(aq)}$ and $NH_4^+{}_{(aq)}$ on the other hand show similar adsorption characteristics on both Pd/Al_2O_3 and Pt/Al_2O_3. The vibrational spectrum of the NO_2^- ion changed substantially upon adsorption, clearly indicating that NO_2^- chemisorbs onto the supported metal catalysts. On the contrary, adsorption of NH_4^+ does not lead to significant change in the vibrational spectrum of the ion, indicating that the NH_4^+ ion does not chemisorb on the noble metal but is stabilized via an electrostatic interaction. When comparing the adsorption of hydroxylamine ($NH_2OH_{(aq)}$) on Pd/Al_2O_3 and Pt/Al_2O_3, significant differences were observed. On Pd/Al_2O_3, hydroxylamine is converted into a stable $NH_{2(ads)}$ fragment, whereas on Pt/Al_2O_3 hydroxylamine is converted into NO, possibly via $HNO_{(ads)}$ as an intermediate.

Introduction

Waste- and groundwater treatments are retrieving more and more attention because of increasing pollution of groundwater.[1] Water purification in general includes both oxidative treatments and hydrogenation processes for organic and inorganic pollutants.[2] Denitrification, such as nitrite and nitrate hydrogenation, is becoming more important due to the high nitrite and nitrate levels found in groundwater in Europe, which in some cases exceeds legal limits, and local wells had to be closed.[1,3] Hydrogenation of nitrate and nitrite over noble metal catalysts was for the first time reported in 1989.[4] Nitrate was reported to first hydrogenate to nitrite, which in turn converted into nitrogen and ammonia. Several authors have proposed a reaction scheme including adsorbed NO as the key intermediate for the catalytic hydrogenation of nitrate and nitrite[5−8] over supported bimetallic catalysts as schematically represented in Scheme 1. Experimental evidence for the presence of the proposed intermediates and products in solution is limited so far to NO_2^-, N_2, and NH_4^+.[6,7,9−11] Moreover, the proposed adsorbed species were never directly observed.

In electrochemical research, electrocatalytic reaction of inorganic nitrogen compounds on transition metals is a classical topic. The electrochemical reduction of nitrate was shown to be more complex than the catalytic hydrogenation shown in Scheme 1.[7,8] Electrochemical reduction has been mainly investigated on platinum electrodes, and this has indicated the presence of a variety of intermediates such as NO_2, HNO_2, NO, N_2O, N_2, H_2-NO, HNO, NH_2OH, and NH_3, depending on reaction conditions.[12−26] Similar to the heterogeneous catalytic reaction, the rate-determining step is the reduction of nitrate to nitrite, which in turn yields adsorbed NO.[17−26] Several papers report on the experimental evidence of adsorbed NO as an intermediate during electroreduction of nitrate and nitrite.[12,14−18] The subsequent electroreduction of adsorbed NO mainly yielded ammonia, while traces of N_2O were also detected. In addition, N_2O was demonstrated to be an intermediate for the production of nitrogen from nitrate on platinum electrodes.[20,27]

* To whom correspondence should be addressed. E-mail: L.Lefferts@utwente.nl.

† Present address: Fuel Cells and Solid State Chemistry Department, Risø National Laboratory, Technical University of Denmark − DTU, Frederiksborgvej 399, DK-4000 Roskilde, Denmark. E-mail: sune.ebbesen@risoe.dk.

(1) World Health Organization. *Water and Health in Europe*; Copenhagen, 2002.

(2) Pintar, A. *Catal. Today* **2003**, *77*, 451−465.

(3) World Health Organization. *Nitrate and Nitrite in Drinking Water*; Copenhagen, 2003.

(4) Vorlop, K. D.; Tacke, T. *Chem. Ing. Tech.* **1989**, *61*, 836.

(5) Daub, K.; Emig, G.; Chollier, M. J.; Callant, M.; Dittmeyer, R. *Chem. Eng. Sci.* **1999**, *54*, 1577−1582.

(6) Daum, J.; Vorlop, K. D. *Chem. Eng. Tech.* **1999**, *22*, 199−202.

(7) Pintar, A.; Batista, J.; Levec, J.; Kijiuchi, T. *Appl. Catal., B* **1996**, *11*, 81−98.

(8) Prüsse, U.; Hahnlein, M.; Daum, J.; Vorlop, K. D. *Catal. Today* **2000**, *55*, 79−90.

(9) Wärnå, J.; Turunen, I.; Salmi, T.; Maunula, T. *Chem. Eng. Sci.* **1994**, *49*, 5763−5773.

(10) Vorlop, K. D.; Prüsse, U., *Environ. Catal.* **1999**, 195.

(11) Hörold, S.; Tacke, T.; Vorlop, K. D. *Environ. Technol.* **1993**, *14*, 931−939.

(12) Gomez, R.; Rodes, A.; Orts, J. M.; Feliu, J. M.; Perez, J. M. *Surf. Sci.* **1995**, *342*, L1104−L1110.

(13) Rodes, A.; Gomez, R.; Orts, J. M.; Feliu, J. M.; Aldaz, A. *J. Electroanal. Chem.* **1993**, *359*, 315−323.

(14) Rosca, V.; Koper, M. T. M. *J. Phys. Chem. B* **2005**, *109*, 16750−16759.

(15) Rosca, V.; Beltramo, G. L.; Koper, M. T. M. *Langmuir* **2005**, *21*, 1448−1456.

(16) Weaver, M. J.; Zou, S. Z.; Tang, C. *J. Chem. Phys.* **1999**, *111*, 368−381.

(17) da Cunha, M. C. P. M.; Weber, M.; Nart, F. C. *J. Electroanal. Chem.* **1996**, *414*, 163−170.

(18) da Cunha, M. C. P. M.; De Souza, J. P. I.; Nart, F. C. *Langmuir* **2000**, *16*, 771−777.

(19) de Groot, M. T.; Koper, M. T. M. *J. Electroanal. Chem.* **2004**, *562*, 81−94.

(20) de Vooys, A. C. A.; Koper, M. T. M.; van Santen, R. A.; van Veen, J. A. R. *Electrochim. Acta* **2001**, *46*, 923−930.

(21) Dima, G. E.; de Vooys, A. C. A.; Koper M. T. M. *J. Electroanal. Chem.* **2003**, *554−555*, 15−23.

(22) Heckner, H. N. *J. Electroanal. Chem.* **1973**, *44*, 9−20.

(23) Nishimura, K.; Machida, K.; Enyo, M. *Electrochim. Acta* **1991**, *36*, 877−880.

(24) Petrii, O. A.; Safonova, T. A. *J. Electroanal. Chem.* **1992**, *331*, 897−912.

(25) Silva, S.; Sottomayor, M. J.; Martins, A. *Electrochim. Acta* **1994**, *39*, 491−496.

(26) van der Plas, J. F.; Barendrecht, E. *Electrochim. Acta* **1980**, *25*, 1463−1469.

(27) Bae, I. T.; Barbour, R. L.; Scherson, D. A. *Anal. Chem.* **1997**, *69*, 249−252.

Scheme 1.   Scheme of Nitrate (and Nitrite) Hydrogenation over Bimetallic Platinum or Palladium Catalysts from Refs 7 and 8
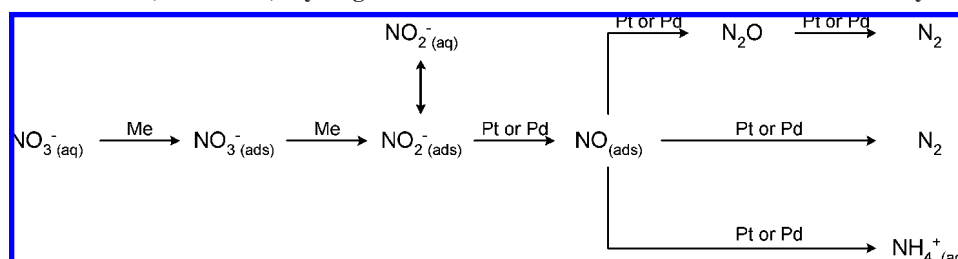
Unfortunately, the insights obtained from electrochemical studies with Fourier transform infrared (FT-IR) spectroscopy cannot directly be compared to catalytic studies because of three reasons. First, FT-IR spectra from the surface of a working electrode can only be obtained when operating with very thin liquid layers between the electrode and the spectrometer window, inducing severe mass transfer problems during experiments. Second, a comparison of electrochemical studies with the results in the present study is difficult, because of the applied potential in electrochemistry. In fact, to do so, one would need IR spectra of adsorbed species at the open circuit potential of a reacting electrode, which, to the best of our knowledge, are not available. Third, electrochemical studies are typically performed on dense conducting electrodes, often single crystals, which are definitely different from practical catalysts containing nanoparticles on porous (nonconducting) support materials. Moreover, it is very difficult to study heterogeneous catalysts in situ if the reaction is carried out in water; thus, detailed mechanistic studies of the heterogeneous catalytic hydrogenation of both nitrate and nitrite over supported noble metal catalysts are lacking.

Attenuated total reflection infrared (ATR-IR) spectroscopy is ideally suited for studying molecular vibrations at the solid−liquid interface because the evanescent wave is restricted to the region near the interface, thereby minimizing the contribution from the liquid.[28] ATR-IR spectroscopic studies at the metal−liquid interface have only recently started to receive attention.[29−35] For example, the adsorption and oxidation of CO and the dissociation of small molecules such as formaldehyde over Pt/Al$_2$O$_3$ catalysts were reported.[33] In addition, ATR spectroscopic studies of the water−gas shift reaction and methanol reforming over Pt/Al$_2$O$_3$ was combined with kinetic studies.[31] Recently, we have demonstrated the benefit of ATR-IR spectroscopy to study in situ the development of adsorbates on supported noble metal catalysts when performing liquid phase reactions in water.[36] In addition, we showed for CO oxidation over Pt/Al$_2$O$_3$ that the properties of the adsorbed intermediate species are significantly altered by the presence of liquid water compared to gas phase or electrochemical CO oxidation.[36]

Because of the promise of ATR-IR for studying in situ formation of adsorbates on supported noble metal catalysts in water, we started a detailed study of the reaction mechanisms of nitrite and nitrate reduction over supported metal catalysts.

It is the objective of this paper to clarify the spectral properties of adsorbed N$_x$O$_y$H$_z$ species on both Pt/Al$_2$O$_3$ and Pd/Al$_2$O$_3$ produced from the adsorption of model compounds. The details of nitrite hydrogenation over both catalysts can be found in ref 37 and will be published in subsequent papers.

Experimental Section

Catalyst Preparation. *Al$_2$O$_3$ Support.* As a support material, γ-Al$_2$O$_3$ (γ-aluminum oxide C, Degussa, primary particle size 13 nm) was used. It was precalcined for 5 h at 823 K (heating rate 5 K/min) in stagnant air before the noble metals were deposited.

The γ-Al$_2$O$_3$ support was also immobilized onto an ATR crystal to perform reference experiments of adsorbed species. It appeared necessary to pretreat the alumina, mimicking the calcination step in the preparation of the palladium and platinum catalysts, to obtain a stable thin layer of alumina. For this reason, a suspension was made of 10 g of precalcined Al$_2$O$_3$ in 200 mL of water and stirred for 2 h at room temperature, followed by drying at 335 K for 2 h in a rotating evaporator. Subsequently, the Al$_2$O$_3$ powder was calcined at 673 K for 2 h (heating rate 5 K/min) in synthetic air (30 mL/min), after which it could be immobilized on an ATR crystal (see below).

Pt/Al$_2$O$_3$. The precalcined γ-Al$_2$O$_3$ powder was impregnated with a solution of H$_2$PtCl$_6$·6H$_2$O (Alfa Aesar) to yield a catalyst with 5 wt % platinum loading (details can be found in a previous paper).[36] The slurry was mixed for 2 h, followed by drying at 335 K for 2 h in a rotating evaporator. The impregnated Pt/Al$_2$O$_3$ powder was then calcined at 673 K for 3 h (heating rate 5 K/min) in synthetic air (30 mL/min) and reduced at 673 K for 3 h (heating rate 5 K/min) in hydrogen (30 mL/min).

Pd/Al$_2$O$_3$. To obtain highly dispersed palladium particles, palladium acetylacetonate (Pd(acac)$_2$) (Alfa Aesar) was adsorbed on the precalcined γ-Al$_2$O$_3$ powder. Adsorption was performed from a solution of Pd(acac)$_2$ in toluene to yield a catalyst with 5 wt % palladium loading. An amount of 1.95 g of Pd(acac)$_2$ (large excess to obtain 5 wt % Pd/Al$_2$O$_3$ catalyst) was dissolved in 400 mL of toluene, and 10 g of precalcined γ-Al$_2$O$_3$ was added and stirred for 24 h at room temperature. The mixture was filtered and dried at 323 K for 15 h in stagnant air, followed by calcination at 573 K (heating/cooling rate 1 K/min) in synthetic air (30 mL/min). To obtain a metal loading of 5 wt % palladium, this procedure was repeated five times with the remaining filtrate from the first adsorption. Subsequently, the calcined catalyst was reduced at 323 K for 2 h (heating/cooling rate 1 K/min) in hydrogen (30 mL/min), followed by flushing with argon (30 mL/min) at 600 K for 1 h (heating/cooling rate 1 K/min) to avoid the presence of any palladium hydride.

Catalyst Characterization. The elemental composition of the powder catalysts was determined with X-ray fluorescence (XRF) spectroscopy using a Phillips PW 1480 spectrometer.

Platinum dispersion was determined with H$_2$ chemisorption using 0.2 g of catalyst in a home-built volumetric system. The sample was reduced at 473 K in H$_2$ for 1 h. After reduction, the sample was degassed at 473 K in vacuum (10^{-6} mbar). The sample was cooled to room temperature (293 K) in vacuum, and the H$_2$ adsorption isotherm was measured. After the first isotherm, the sample was

(28) Harrick, N. J. *Internal Reflection Spectroscopy*; Interscience Publishing: New York, 1967.

(29) Bürgi, T.; Baiker, A. *J. Phys. Chem. B* **2002**, *106*, 10649−10658.

(30) Ebbesen, S. D.; Mojet, B. L.; Lefferts, L. *Langmuir* **2006**, *22*, 1079−1085.

(31) He, R.; Davda, R. R.; Dumesic, J. A. *J. Phys. Chem. B* **2005**, *109*, 2810−2820.

(32) Kizhakevariam, N.; Jiang, X.; Weaver, M. J. *J. Chem. Phys.* **1994**, *100*, 6750−6764.

(33) Ortiz-Hernandez, I.; Williams, C. T. *Langmuir* **2003**, *19*, 2956−2962.

(34) Yee, N. C.; Chottiner, G. S.; Scherson, D. A. *J. Phys. Chem. B* **2005**, *109*, 7610−7613.

(35) Bürgi, Y.; Baiker, A. *Adv. Catal.* **2006**, *50*, 227−283.

(36) Ebbesen, S. D.; Mojet, B. L.; Lefferts, L. *J. Catal.* **2007**, *246*, 66−73.

(37) Ebbesen, S. D. Spectroscopy under the Surface−In-Situ ATR-IR Studies of Heterogeneous Catalysis in Water. Doctoral Thesis, separate chapters are in preparation for publication, Gildeprint BV, Enschede, 2007.

degassed at room temperature, followed by a second H_2 adsorption isotherm. The hydrogen chemisorption capacity (H/Pt) was calculated by extrapolation of the hydrogen uptake to zero pressure, which corresponded to the difference of the first and second isotherms.[38]

Palladium dispersion was determined with CO chemisorption of 0.15 g of catalyst in a dynamic system (ChemiSorb 2750, Micromeritics). The sample was reduced at 323 K in H_2 for 1 h (heating rate 1 K/min). After reduction, the sample was purged with argon at 323 K and cooled to room temperature. Subsequently, pulses of 0.1 mL of CO were introduced to the sample until zero uptake (around 10 pulses). CO uptake was monitored by a thermal conductivity detector (TCD). The dispersion and palladium surface area were calculated assuming stoichiometric adsorption of one CO molecule per palladium surface atom.

The Brunauer−Emmett−Teller (BET) specific surface area of the powders was measured with N_2 adsorption−desorption at 77 K in an ASAP 2400 (Micromeretics) instrument.

The structure of the layers deposited on the IRE was studied with scanning electron microscopy (SEM) (LEO 1550 FEG SEM). Since it was too costly to break the ATR crystals for examination, the preparation of the sample layers was mimicked on a glass plate. The glass plate was cut through from the back side using a diamond cutter, and the sample layer was carefully broken and studied by SEM.

Preparation of Thin Catalyst Layers on the Internal Reflection Element (IRE). Suspensions of either Al_2O_3, Pt/Al_2O_3, or Pd/Al_2O_3 were prepared from their respective powders (0.10 g of Al_2O_3, 0.3 g of Pt/Al_2O_3, or 0.15 g of Pd/Al_2O_3) in 50 mL of water; the pH was adjusted to 3.5 with nitric acid to stabilize the small alumina particles. Different amounts of powders were used, since this appeared to be necessary to prevent cracking of the final layer. Each suspension was milled for 1 h in a ball-mill (Fritsch Pulverisette) to obtain Al_2O_3 particles of a few nanometers in size. Subsequently, colloidal alumina (aluminum oxide, 20% in H_2O colloidal suspension, Alfa Aesar, particle size 5 nm) was added, which is the general methodology of preparing wash coats in monolithic catalysts.[39] For preparation of the Al_2O_3 layer, 0.025 mL of colloidal alumina was added, whereas, respectively, 0.075 and 0.0375 mL were added for the Pt/Al_2O_3 and Pd/Al_2O_3 suspensions (each corresponding to 5 wt % of the catalyst amount).

Each catalyst layer was prepared on a ZnSe IRE by adding 1 mL of the catalyst/water suspension evenly on one side of the IRE. The suspension was allowed to evaporate overnight at room temperature. Subsequently, the catalyst layer/IRE was heated to 573 K for 2 h (heating rate 1 K/min) in flowing argon to ensure removal of all NO_x species on the catalyst surface. The procedure had to be repeated twice for the Al_2O_3 layer and once for the Pd/Al_2O_3 layer to limit the formation of cracks in the final catalyst layer. About 6 mg of catalyst was deposited on the IRE in all cases. Further, an additional reduction treatment was necessary for Pt/Al_2O_3 to remove all NO_x species (heating to 673 K in hydrogen, heating/cooling rate 10 K/min).

In Situ ATR-IR Spectroscopy. The water used in all ATR-IR experiments was ultrapure Q2-water, prepared with a Millipore Milli-Q water treatment system from Amphotech Ltd. Saturation of water with Ar (5.0, Praxair), 10% O_2/Ar (5.0, Praxair), or H_2 (5.0, Praxair) was performed at room temperature (294 K) with gas flow rates of 40 mL/min for 2 h. Prior to saturation with O_2 or H_2, air was removed by saturation with argon for at least 2 days. The concentrations of dissolved gases in water were calculated based on reported solubility data at room temperature and 1 atm gas pressure.[40] The Q2-water saturated with Ar (2.3×10^{-3} mol/L), O_2 (1.3×10^{-4} mol/L), or H_2 (4.1×10^{-4} mol/L) is designated in the following as Ar/H_2O, O_2/H_2O, or H_2/H_2O, respectively.

Solutions of $NH_4^+{}_{(aq)}$ (4.3×10^{-4} mol/L), $NH_2OH_{(aq)}$ (4.3×10^{-4} mol/L $NH_2OH \cdot HCl$, pH 5), $NO_2^-{}_{(aq)}$ (4.3×10^{-4} mol/L), and $NO_3^-{}_{(aq)}$ (4.3×10^{-4} mol/L) were prepared in Ar/H_2O from NH_4Cl (99.999%,

Alfa Aesar), $NH_2OH \cdot HCl$ (99%, Alfa Aesar), $NaNO_2$ (Merck), and $NaNO_3$ (Aldrich), respectively. For each solution, the pH was adjusted to pH 7 by adding either HCl (37%, Merck) or NaOH (Merck); the pH was measured using a pH meter (744 pH meter, Metrohm).

ATR-IR spectra were recorded using a home-built stainless steel flow-through cell as described elsewhere.[38] The flow-through chamber was created by a spacer placed between the polished steel top-plate and the IRE. The thickness of the spacer was 0.3 mm, and the length and width of the exposed area of the coated IRE was 40 × 10 mm^2, respectively. The total volume of the cell was 120 μL. The liquid flow rate was 1 mL/min in all experiments; as a result, the residence time in the cell was 7.2 s. For each adsorption experiment, a freshly prepared sample layer was used.

The cell was mounted in the sample compartment of an infrared spectrometer (Bruker Tensor 27) equipped with a mercury cadmium telluride (MCT) detector. After assembling the cell in the IR spectrometer, the cell was flushed with Ar/H_2O until a stable water spectrum was obtained. The ATR-IR spectra were recorded at room temperature (294 K) in an air-conditioned room, by averaging of 128 scans taken with a resolution of 4 cm^{-1} during 70 s; spectra started with 90 s intervals.

Data Treatment. As shown recently by our group, it is necessary to correct the ATR-IR spectra for the infrared absorbance of water.[30] Details on the subtraction of a scaled background for dissolved gases can be found in the same reference. After subtraction of the water spectra, the residual spectra showed a complexity of peaks. For this reason, curve fitting was applied using a Lorentzian function. The applied Lorentzian line-shape function centered at the frequency ω_0 is given by

$$I(\omega) = A\frac{2}{\pi}\frac{w}{4(\omega - \omega_0) + w^2} \tag{1}$$

with $I(\omega)$ being the intensity at a given frequency ω, A being the integrated area, and w being the full width at half of the maximum intensity.

Results

Catalyst Characterization. The total surface area of the γ-Al_2O_3 support powder after precalcination at 823 K was 125 m^2/g as determined by N_2 physisorption. Deposition of palladium or platinum caused a slight decrease of the total surface area to 115 m^2/g. The thickness of the layer was examined on samples prepared on a glass plates; cutting allowed microscopic investigation of a cross section of the thin layer.

Figure 1a shows typical SEM micrographs of the γ-Al_2O_3 layer on the glass plate. The thickness of the catalyst layer was 6.5 ± 0.5 μm over the full length of the plate. As can be seen on the right side in Figure 1a, the layer contained some cracks. Nevertheless, layers on the IRE appeared stable during aqueous flow over several days. Based on the layer thickness and the catalyst amount, the void fraction between catalyst particles was calculated to be 35%.

Figure 1b shows SEM micrographs of a thin layer of 5 wt % Pd/Al_2O_3 on a glass plate. The layer consisted of small particles of typically a few nanometers, and the layer showed some small cracks, like the Al_2O_3 layer. The thickness of the Pd/Al_2O_3 layer was 5.0 ± 0.5 μm, resulting in a void fraction of 25%. The thickness of the Pt/Al_2O_3 layer (not shown) was 3.50 ± 0.25 μm (void fraction 10%) over the full length of the plate, in agreement with our previous work.[36] Table 1 summarizes the characterization data of the samples.

In Situ ATR-IR Spectroscopy. *$NO_2^-{}_{(aq)}$ Adsorption.* Figure 2a shows the ATR-IR spectra obtained after 15 min of flowing with a solution of $NO_2^-{}_{(aq)}$ on a clean ZnSe IRE and layers of Al_2O_3, Pd/Al_2O_3, and Pt/Al_2O_3. For both ZnSe and Al_2O_3, one distinct peak is observed at 1235 cm^{-1}. On Pt/Al_2O_3 and $Pd/$

(38) Benson, J. E.; Hwang, H. S.; Boudart, M. *J. Catal.* **1965**, *4*, 704−710.

(39) Nijhuis, T. A.; Beers, A. E. W.; Vergunst, T.; Hoek, I.; Kapteijn, F.; Moulijn, J. *Catal. Rev. − Sci. Eng.* **2001**, *43*, 345-

(40) Weast , R. C., Ed. *Handbook of Chemistry and Physics*, 48th ed.; The Chemical Rubber CO: Cleveland, OH, 1970.
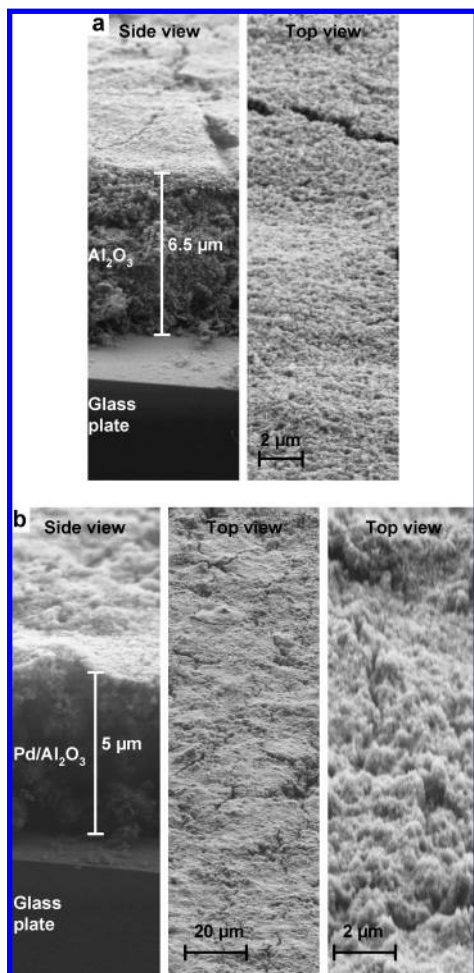
Figure 1. SEM micrographs of (a) Al_2O_3 and (b) Pd/Al_2O_3 on a glass plate with identical dimensions as the ZnSe IRE (left: side view and right: top view).

Al_2O_3, also additional peaks are found at 1390 and 1305 cm^{-1} (Pt/Al_2O_3) and 1405 and 1325 cm^{-1} (Pd/Al_2O_3). In addition, small shoulders at 1460 cm^{-1} (Pt/Al_2O_3) and 1475 cm^{-1} (Pd/Al_2O_3) were observed on the noble metal catalysts.

Subsequent flow with Ar/H_2O removed the species giving rise to the peak at 1235 cm^{-1} for all samples within the 90 s data acquisition time. Since for Al_2O_3 and clean ZnSe no signals were observed, Figure 2b shows the resulting spectra for Pt/Al_2O_3 and Pd/Al_2O_3 only. For Pd/Al_2O_3, the integrated intensity of the peaks at 1405 and 1325 cm^{-1} remained constant during flushing. However, on Pt/Al_2O_3, a decrease in intensity for the peaks at 1390 and 1305 cm^{-1} was observed as can be seen in Figure 3. Figure 3 shows the evolution of the peaks observed on Pt/Al_2O_3 when flowing $NO_2^-_{(aq)}$ (0−16.5 min) and subsequently Ar/H_2O (16.5−30 min). During nitrite adsorption, a stabilization period is observed of about 10 min, which is typical for these experiments and independent of the catalyst layer. It is due to a chromatographic effect, because of the low flow rate (1 mL/min) and the low concentration of nitrite in the solution. As an example, at least 3 min are needed to introduce sufficient NO_2^- to the catalysts to obtain a NO_2^-/Pt ratio of 1. However, longer flow times will be required if nitrite also adsorbs on the support. The delay is clearly not due to slow diffusion into the catalyst layer, since the peak at 1235 cm^{-1} disappears instantaneously (that means within 90 s, which is the time resolution of the experiment) when flowing Ar/H_2O. During Ar/H_2O flow, a slight decrease in the integrated intensity of the peak at 1390 cm^{-1} was detected, while the intensity

of the 1305 cm^{-1} peak decreased much more rapidly to about 70% of its original intensity after 14 min.

$NH_4^+_{(aq)}$ *Adsorption.* Figure 4 shows the ATR-IR spectra obtained after a 15 min flow of $NH_4^+_{(aq)}$ over a clean ZnSe IRE and layers of Al_2O_3, Pd/Al_2O_3, and Pt/Al_2O_3. In all spectra, one evident peak was found at 1455 cm^{-1} (ZnSe, Al_2O_3, Pt/Al_2O_3) or 1450 cm^{-1} (Pd/Al_2O_3) with similar peak widths between 60 and 70 cm^{-1}. Evidently, the intensity of the peaks was quite different, as can be concluded from the scaling factors used in Figure 4. The intensity and peak position were completely reproducible for all samples. Since the observed intensity is a function of layer thickness, porosity, adsorption state (if any), surface oxidation degree, and extinction coefficient, only the peak positions for NH_4^+ on the different catalysts will be used from here on. During subsequent Ar/H_2O flow, the peak instantaneously (within 90 s) disappeared from the ZnSe and Al_2O_3 spectra. The peaks appeared much more stable on Pt/Al_2O_3 and Pd/Al_2O_3; the integrated intensities decreased by only 5% and 15%, respectively, in 90 s, whereas the peak positions did not change at all. Interestingly, subsequent exposure to H_2/H_2O completely removed the peaks on Pd/Al_2O_3 and Pt/Al_2O_3 within 90 s (not shown).

$NH_2OH_{(aq)}$ *Adsorption.* When adsorbing $NH_2OH_{(aq)}$ (hydroxylamine), disproportionation into ammonia, nitrous oxide, and nitrogen has to be taken into account.[41,42] As a typical example, Figure 5 shows the spectrum of Pt/Al_2O_3 after flowing a hydroxylamine solution at pH 7. A clear peak is observed at 1455 cm^{-1}, similar to the peak observed after adsorption of ammonia (Figure 4), together with a shoulder at 1550 cm^{-1}. In addition, a clear peak at 2231 cm^{-1} was found, which can be attributed to N_2O, since bulk N_2O is characterized by a N−N stretching vibration at 2224 cm^{-1} (ref 43) and peaks around 2230 cm^{-1} are generally assigned to N_2O.[18,27,44,45]

The rate of the disproportionation reaction is known to decrease with decreasing pH. As the ZnSe crystal will start to corrode at pH 4, additional experiments were performed at pH 5, attempting to suppress the disproportionation of hydroxylamine without dissolving the IRE.

Figure 6 shows ATR-IR spectra after flowing $NH_2OH_{(aq)}$ at pH 5 over Pd/Al_2O_3 and Pt/Al_2O_3. Clearly, both catalysts showed signals of adsorbed species but at different frequencies. During adsorption of $NH_2OH_{(aq)}$ on Al_2O_3 as well as on clean ZnSe, no adsorption bands were observed. On Pd/Al_2O_3, a broad asymmetric peak was found at 1510 cm^{-1}, which could be deconvoluted into two peaks positioned at 1510 and 1450 cm^{-1} (see Figure 6c). The peak intensities and positions remained constant during both subsequent Ar/H_2O flow and subsequent O_2/H_2O flow.

For Pt/Al_2O_3, a broad peak at 1540 cm^{-1} with a shoulder on each side was detected. This overall signal was composed of three well-defined peaks at 1575, 1540, and 1455 cm^{-1} (Figure 6b). Moreover, for Pt/Al_2O_3 also a peak at 2231 cm^{-1} was found, which was absent on Pd/Al_2O_3. Contrary to the stable signals on Pd/Al_2O_3, for Pt/Al_2O_3, the spectra significantly changed during Ar/H_2O flow after hydroxylamine adsorption as can be seen in Figure 7. The peak at 2231 cm^{-1} quickly disappeared within 90 s during Ar/H_2O flow, while the peak at 1540 cm^{-1} seemed to shift to 1580 cm^{-1}. Deconvolution of the signal, however, again

(41) Moews, P. C.; Audrieth, L. F. *J. Inorg. Nucl. Chem.* **1959**, *11*, 242−246.
(42) van de Moesdijk, C. G. M. The Catalytic Reduction of Nitrate and Nitric Oxide to Hydroxylamine: Kinetics and Mechanism. Doctoral Thesis, Technische Hogeschool, Eindhoven, 1979.
(43) Begun, G. M.; Fletcher, W. H. *J. Chem. Phys.* **1958**, *28*, 414−418.
(44) Rodes, A.; Gomez, R.; Orts, J. M.; Feliu, J. M.; Perez, J. M.; Aldaz, A. *Langmuir* **1995**, *11*, 3549−3553.
(45) Rosca, V.; Beltramo, G. L.; Koper, M. T. M. *J. Electroanal. Chem.* **2004**, *566*, 53−62.

Table 1. Characterization of the Al_2O_3, Pd/Al_2O_3, and Pt/Al_2O_3 Layers

	metal content	metal dispersion	accessible metal/g catalyst (mmol)	layer thickness (μm)	BET surface area (m^2/g)	void fraction (%)
Al_2O_3				6.5 ± 0.5	125	35
Pt/Al_2O_3	5.0 wt % Pt	0.75^b	0.192	3.5 ± 0.25	115	10
Pd/Al_2O_3	5.0 wt % Pd	0.45^a	0.206	5.0 ± 0.5	11	25

^{a} Palladium dispersion was determined by CO chemisorption assuming CO/Pd = 1. ^{b} Platinum dispersion was determined by H_2 chemisorption assuming H/Pt = 1.
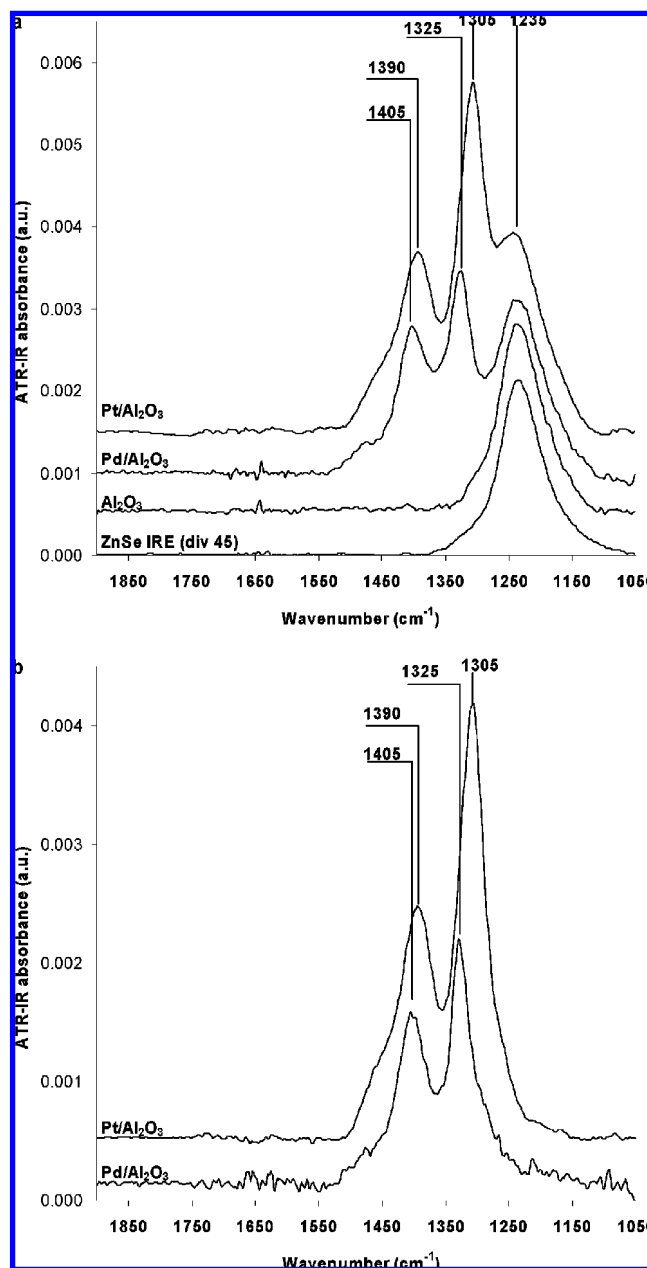

Figure 2. Water corrected ATR-IR spectra from 1900 to 1050 cm^{-1} (a) after 15 min flow of a solution of 4.3×10^{-4} mol/L $NO_2^-_{(aq)}$ at pH 7 and (b) after subsequent flow of Ar/H_2O over Pd/Al_2O_3 and Pt/Al_2O_3.

Figure 3. Integrated peak areas during adsorption of $NO_2^-_{(aq)}$ and during subsequent inert flow over Pt/Al_2O_3.
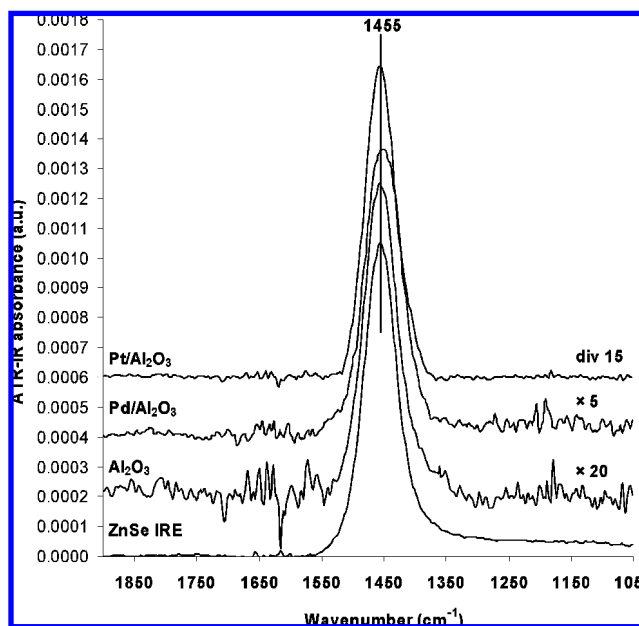
Figure 4. Scaled, water corrected ATR-IR spectra obtained while a solution of 4.3×10^{-4} mol/L NH_4^+ was flown over Pt/Al_2O_3, Pd/Al_2O_3, Al_2O_3, and a clean ZnSe IRE (2.5×10^{-2} mol/L NH_4^+).

revealed the presence of two peaks at 1540 and 1575 cm^{-1}, with the latter shifting to 1580 cm^{-1} with increasing time, while the 1540 cm^{-1} peak did not shift but only decreased in intensity. On the other hand, the peak at 1455 cm^{-1} remained constant. The evolution of the intensities of the peaks at 1540 and 1575 cm^{-1} with time is shown in Figure 7b. Figure 7b clearly shows that the decrease in in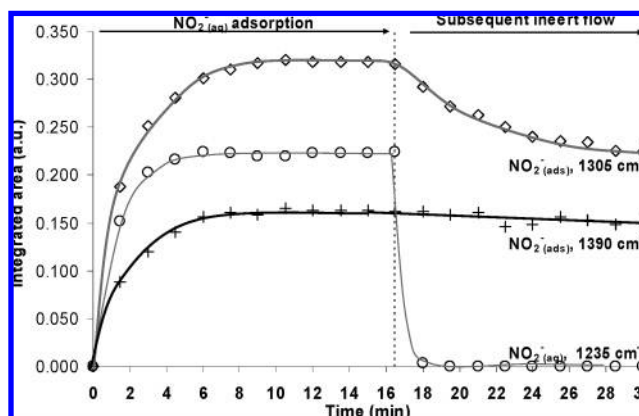tensity of the peak at 1540 cm^{-1} is accompanied by a simultaneous increase of the peak at 1575−1580 cm^{-1}. Both signals stabilize after approximately 20 min of Ar/H_2O flow.

To examine the stability of the species at 1540 cm^{-1} toward oxygen, NH_2OH was adsorbed on Pt/Al_2O_3 and subsequently O_2/H_2O was introduced to the cell while ATR-IR spectra were recorded (Figure 8). Similar to the experiment with Ar/H_2O flow (Figure 7), the peak at 2231 cm^{-1} disappeared instantaneously. However, the signal at 1540 cm^{-1} diminished in about 15 min and a new peak at 1305 cm^{-1} appeared concurrently. A similar peak at 1305 cm^{-1} was also observed during NO_2^- adsorption on Pt/Al_2O_3, although with a much higher intensity (see Figure 2).
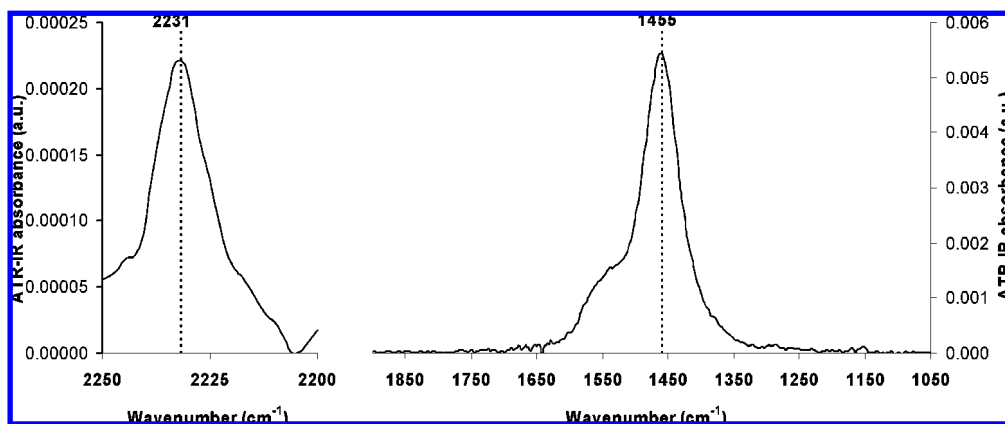
Figure 5. Water corrected ATR-IR spectra after a flow of 4.3×10^{-4} mol/L $NH_2OH_{(aq)}$ over Pt/Al_2O_3 at pH 7.

Discussion

The ultimate goal of our work is to study the surface intermediates during the heterogeneous catalytic hydrogenation of nitrite over supported noble metal catalysts.[37] As a first step, this study reports on the spectral properties of adsorbed $N_xO_yH_z$ species on Pt/Al_2O_3 and Pd/Al_2O_3 produced by adsorption of model compounds. In the following, the catalyst characterization and the identification of adsorbed species are discussed.

Catalyst Characterization. The applied method of sample immobilization on an IRE clearly resulted in stable layers which could be applied in flowing aqueous solutions for days. It turned out that the exact method of preparation to obtain a stable layer is different for Pd/Al_2O_3 compared to Pt/Al_2O_3. In the case of Pt/Al_2O_3, the catalyst layer could be prepared by adding the suspension just once, whereas for Pd/Al_2O_3 it was necessary to use half the amount of catalyst for the suspension and repeat the deposition. However, in both cases, the method reported here via application of colloidal alumina followed by calcination and reduction to immobilize the catalyst layer resulted in smooth and stable layers. SEM pictures revealed some cracks in the Al_2O_3 and Pd/Al_2O_3 layers (Figure 1), but this did not affect the stability, since intensities during the ATR-IR experiments remained constant.

Interestingly, although the layers were prepared in a similar way by adding colloidal alumina, the void fraction in the catalyst layers differed significantly (see Table 1). For Pt/Al_2O_3, the void fraction was 10%, indicating a denser layer compared to Pd/Al_2O_3 which had a void fraction of 25%. The Al_2O_3 layer showed an even higher void fraction. For some reason, the efficiency of catalyst particle packing is different due to differences in catalyst preparation. The Pd/Al_2O_3 catalyst was prepared from an organic solution (toluene, see the Experimental section), resulting in a very "fluffy" catalyst powder and thereby a higher void fraction of the layer deposited on the IRE than that obtained for the Pt/Al_2O_3 catalyst. The underlying chemical reasons for these differences and the different methods to prepare stable catalyst layers are unknown and outside the scope of this work.

Dispersion measurements show that both Pt/Al_2O_3 and Pd/Al_2O_3 have similar numbers of accessible surface atoms per gram of catalyst, 0.192 mmol Pt/g and 0.206 mmol Pd/g. All ATR-IR spectra for Pt/Al_2O_3 reported here show, however, integrated intensities that are approximately 1.5–2 times higher than those for Pd/Al_2O_3. It is not reasonable to assume that the extinction coefficient of identical adsorbates on platinum and palladium would differ that much. Also, it is not likely that differences in the penetration depth for both catalyst layers can account for this effect; as shown in the Supporting Information, the calculated penetration depth is only 1.06 times higher for Pt/Al_2O_3 compared to Pd/Al_2O_3. As a consequence, the denser Pt/Al_2O_3 layer has a larger number of surface sites per micrometer of path length, and approximately 1.75 times more metal sites will be probed as compared to Pd/Al_2O_3 (see calculation in the Supporting Information). This agrees well with the 1.5–2 times higher intensities on Pt/Al_2O_3 as compared to Pd/Al_2O_3.

Finally, during layer preparation, heat treatments were applied up to 673 K and sublimation and deposition of ZnSe on the catalyst layer could heavily influence the adsorption properties of the samples. However, since the ATR-IR infrared spectra of the layers after CO adsorption are identical to the transmission FT-IR spectra of the powder samples, sublimation and deposition of ZnSe can be excluded.[36]

$NO_2^-_{(aq)}$ Adsorption. In the literature, several peak positions for the ν_{as} value of the free nitrite ions have been reported, varying between 1235 and 1286 cm^{-1}.[46,47] When flowing a solution of $NO_2^-_{(aq)}$ over a clean ZnSe IRE or an Al_2O_3 layer, single peaks were observed at 1235 cm^{-1} with identical peak widths, which rapidly disappeared during inert Ar/H_2O flow (Figure 2). Consequently, the peak at 1235 cm^{-1} is assigned to free, dissolved $NO_2^-_{(aq)}$. In addition, it can be concluded that NO_2^- does not adsorb strongly on Al_2O_3 under the applied experimental conditions.

Nitrite adsorption on Pd/Al_2O_3 or Pt/Al_2O_3 also showed the presence of free $NO_2^-_{(aq)}$ as indicated by the peak at 1235 cm^{-1}, which quickly disappeared during Ar/H_2O flow (Figure 2). In addition, peaks at higher wavenumbers were found at 1405 and 1325 cm^{-1} (Pd/Al_2O_3) and 1390 and 1305 cm^{-1} (Pt/Al_2O_3), together with small shoulders at 1460 cm^{-1} (Pt/Al_2O_3) and 1475 cm^{-1} (Pd/Al_2O_3) (Figure 2). Clearly, these peaks must be associated with species adsorbed on the metal particles, because the bands were not observed on either ZnSe or Al_2O_3. In addition, the difference in peak position of about 20 cm^{-1} to a higher wavenumber observed for Pd/Al_2O_3 compared to Pt/Al_2O_3 strongly suggests that the adsorbed species are similar in nature on Pd/Al_2O_3 and Pt/Al_2O_3. In general, for a given adsorbed species, observed frequencies on palladium are at a higher wavenumber than on platinum. For example, CO on palladium absorbs at approximately 20 cm^{-1} higher than CO on platinum.[48–53] Similarly, linearly adsorbed NO on Pt(111) in

(46) Hadjiivanov, K. I. *Catal. Rev. − Sci. Eng.* **2000**, *42*, 71−144.

(47) Nakamoto, K. *Infrared Spectra of Inorganic and Coordination Compounds*; Wiley-Interscience: New York, 1970.

(48) Monteiro, R. S.; Dieguez, L. C.; Schmal, M. *Catal. Today* **2001**, *65*, 77−89.

(49) Barth, R.; Pitchai, R.; Anderson, R. L.; Verykios, X. *J. Catal.* **1989**, *116*, 61.
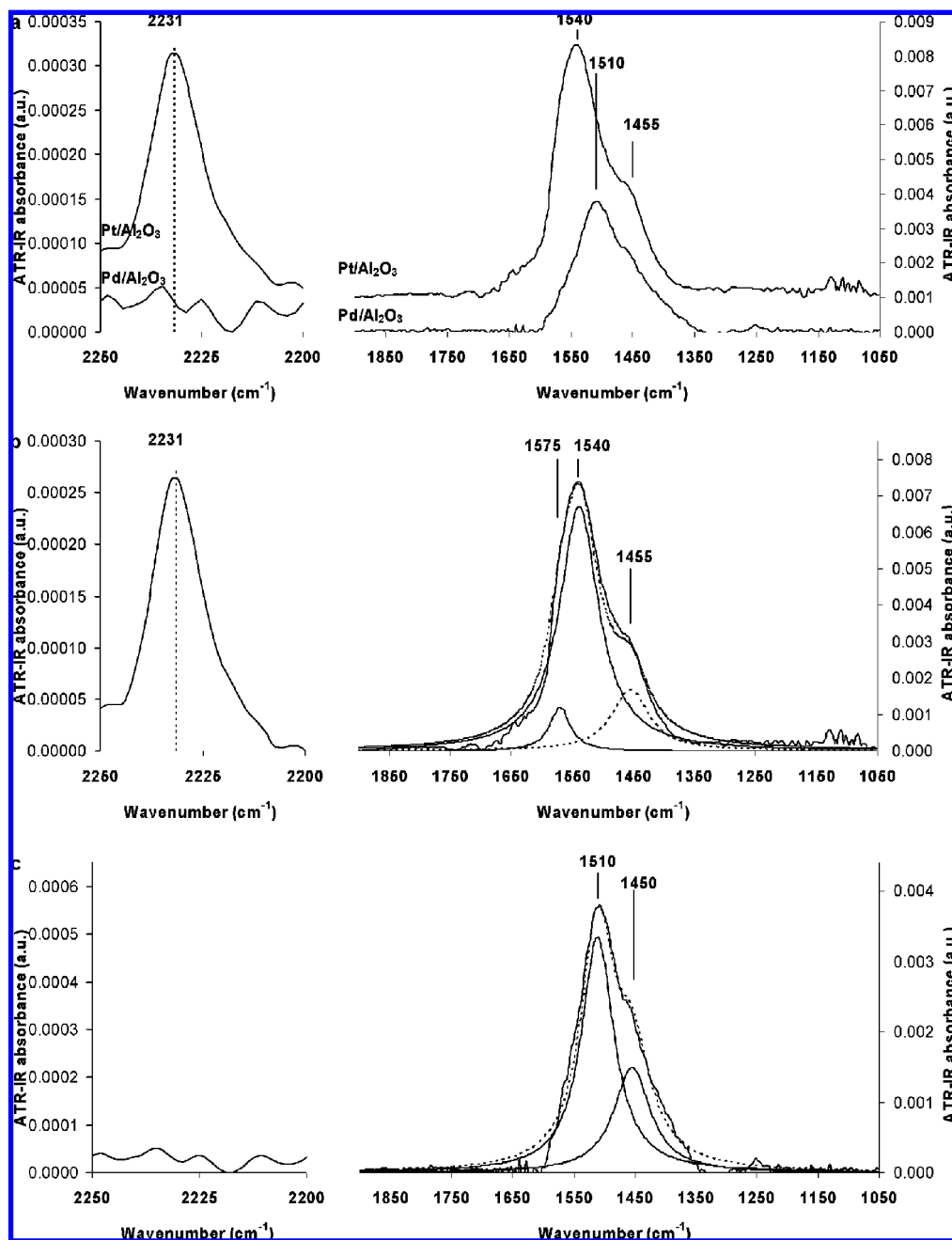
Figure 6. Water corrected ATR-IR spectra during adsorption of $NH_2OH_{(aq)}$ at pH 5 on (a) Pt/Al_2O_3 and Pd/Al_2O_3, and fitted peaks after adsorption on (b) Pt/Al_2O_3 and (c) Pd/Al_2O_3.

water is characterized by a peak at $1660-1680$ cm^{-1},[12,16] whereas linearly adsorbed NO on Pd(111) is located at 1748 cm^{-1}.[54]

Figure 3 shows that during inert flow the ratio of integrated intensities of the two peaks on Pt/Al_2O_3 changed, whereas the intensities remained constant when the same experiment was performed on Pd/Al_2O_3 (not shown). Furthermore, the integrated intensity ratio of the two peaks on each sample varied with pH (not shown). Therefore, the two peaks must be assigned to two different adsorbed species.

It is well-known that nitrite can adsorb in different geometries, which can be divided into two main categories: nitro (coordinated via the nitrogen atom) and nitrito (coordinated by one or two of the oxygen atoms). All of these species have N−O stretch frequencies reported between 1500 and 1200 cm^{-1}; however, there is significant disagreement in the literature concerning the exact assignment.[46] Moreover, infrared frequencies for nitrate species have been reported in the same range. Since the experiments were performed on catalyst surfaces that were passivated during transport through air, the formation of surface nitrates cannot be excluded at this point. Furthermore, the high dispersion of the metal particles indicates that many different crystal planes, steps, and kinks will be present, which provide a variety of metal adsorption sites. From single-crystal studies, it is well-known that each type of adsorption site gives rise to unique metal−adsorbate vibrational properties.

(50) Dulaurent, O.; Chandes, K.; Bouly, C.; Bianchi, D. *J. Catal.* **1999**, *188*, 237−251.
(51) Bourane, A.; Dulaurent, O.; Bianchi, D. *J. Catal.* **2000**, *196*, 115−125.
(52) Skotak, M.; Karpinski, Z.; Juszczyk, W.; Pielaszek, J.; Kepinski, L.; Kazachkin, D. V.; Kovalchuk, V. I.; d'Itri, J. L. *J. Catal.* **2004**, *227*, 11−25.
(53) Bourane, A.; Dulaurent, O.; Bianchi, D. *Langmuir* **2001**, *17*, 5496−5502.
(54) Zou, S.; Gomez, R.; Weaver, M. J. *J. Electroanal. Chem.* **1999**, *474*, 155−166.
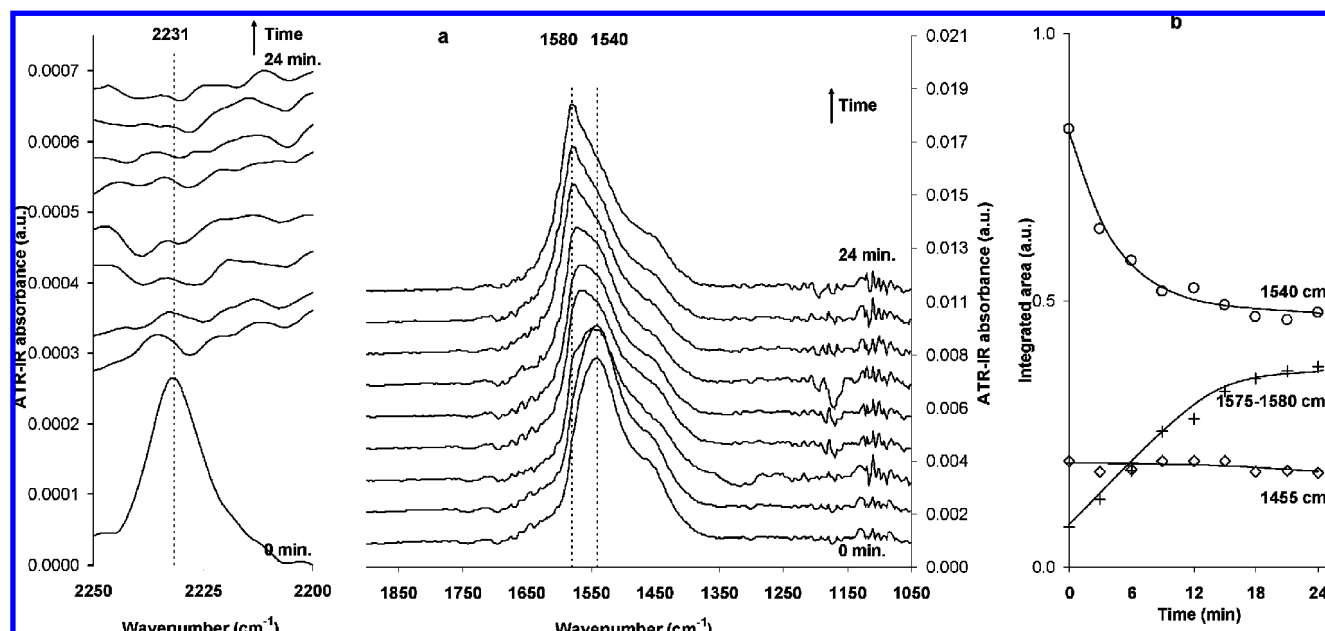
Figure 7. (a) Water corrected ATR-IR spectra during a flow of Ar/H_2O after adsorbing $NH_2OH_{(aq)}$ on Pt/Al_2O_3 and (b) corresponding integrated peak areas.

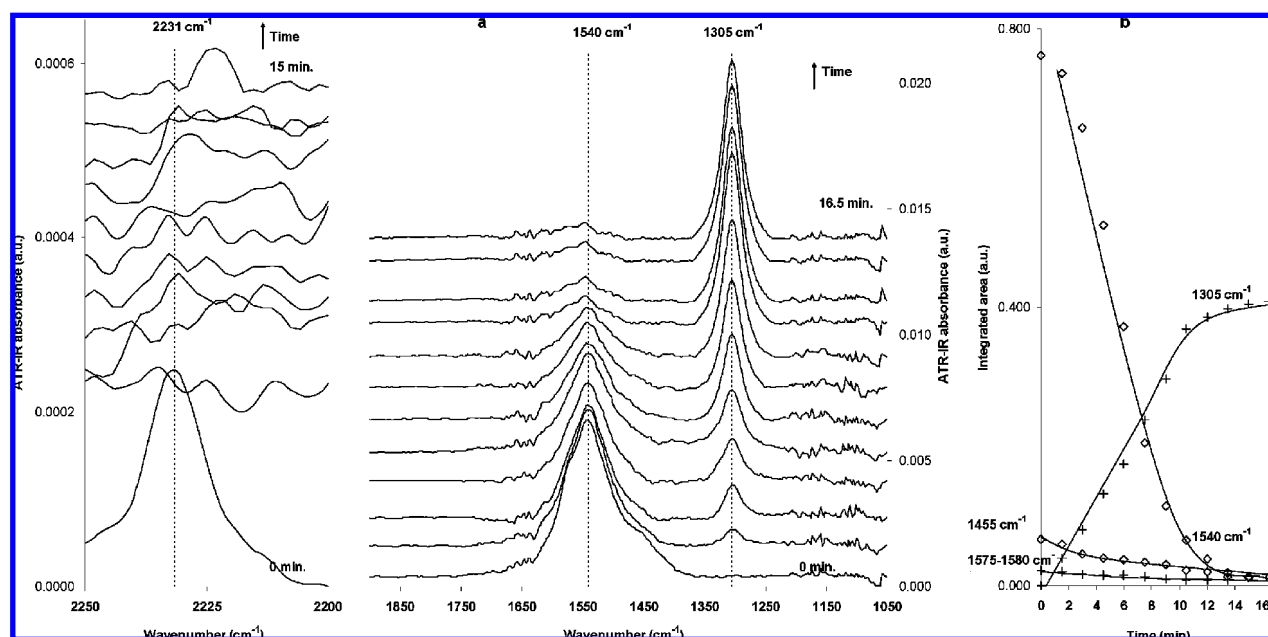
Figure 8. (a) Water corrected ATR-IR spectra during a flow of O_2/H_2O after adsorbing $NH_2OH_{(aq)}$ on Pt/Al_2O_3 and (b) corresponding integrated peak areas.

In conclusion, the peaks at 1405 and 1325 cm^{-1} (Pd/Al_2O_3) and 1390 and 1305 cm^{-1} (Pt/Al_2O_3) and the accompanying shoulders at 1460 cm^{-1} (Pt/Al_2O_3) and 1475 cm^{-1} (Pd/Al_2O_3) are assigned to NO_x^- ($x = 2,3$) species adsorbed on palladium and platinum sites. These species are stable if adsorbed on palladium, and they show different desorption rates if adsorbed on platinum.

$NH_4^+{}_{(aq)}$ Adsorption. A peak at 1455 cm^{-1}, with a peak width of 61 cm^{-1}, was observed when flowing a solution of $NH_4^+{}_{(aq)}$ over a clean ZnSe IRE or an Al_2O_3 layer, which rapidly disappeared during inert Ar/H_2O flow (Figure 4). This band at 1455 cm^{-1} can be assigned to the symmetric bending mode of NH_4^+.[55-57] Its frequency is approximately 30−60 cm^{-1} lower than that in typical ammonium salts, suggesting that NH_4^+ forms strong hydrogen bonds with the surrounding water molecules.[57]

Clearly, NH_4^+ does not adsorb strongly on either ZnSe or Al_2O_3 under the applied experimental conditions, since the band rapidly disappears when flushing with Ar/H_2O. The observation that NH_4^+ does not adsorb on Al_2O_3 is in agreement with the fact that the applied pH (= 7) is below the isoelectric point of Al_2O_3 ($IEP_{Al_2O_3}$ = 8.5).

Adsorption of $NH_4^+{}_{(aq)}$ on Pd/Al_2O_3 or Pt/Al_2O_3 showed similar bands at 1450 and 1455 cm^{-1}, respectively, which decreased by 5% and 15% in intensity, respectively, within 90 s during flushing with Ar/H_2O. A huge and reproducible difference in intensity

(55) Nyquist, R. A.; Kagel, R. O. *Infrared Spectra of Inorganic Compounds*; Academic Press: New York, 1971.
(56) Schumaker, N. E.; Garland, C. W. *J. Chem. Phys.* **1970**, *53*, 392−407.
(57) Zhou, W.; Fukushima, T.; Ito, M. *Sci. Technol. Adv. Mater.* **2006**, *7*, 216−218.

was found for the two catalysts, with the intensity for ammonia adsorbed on Pt/Al₂O₃ being about 75 times higher than that on Pd/Al₂O₃. Because the variations in intensities for the other species in this study are much smaller, it seems that the large difference for adsorbed ammonia has a physical and/or chemical origin, for which neither the literature nor we have an explanation at present.

The small red shift for Pd/Al₂O₃ compared to Pt/Al₂O₃ and the relative high stability of the signals during inert flow indicate that NH_4^+ is interacting with the metal particles. The similarity in peak position, width, and shape between NH_4^+ detected on Al₂O₃ and the catalysts, however, suggests that NH_4^+ is not chemisorbed but is interacting electrostatically as hydrated ions with the noble metal catalysts. Chemisorption would induce a significant change in the vibrational spectrum of the ion, since then H^+ would need to dissociate, resulting in an adsorbed NH_3 fragment. $NH_{3(ads)}$ would show an umbrella mode between 1300 and 1250 cm⁻¹, which was not observed in our experiments.[57] Moreover, introduction of hydrogen (H₂/H₂O) resulted in an instantaneous disappearance of the ammonium signal, most likely caused by reduction of the metal particles. As indicated earlier, the catalysts are passivated in air before mounted into the ATR cell. As a result, the surface of the metal particles is slightly oxidized. This surface oxidation introduces charge separation, and the oxygen atoms on the surface are slightly negatively charged. Obviously, NH_4^+ can be stabilized on this oxide layer electrostatically. As soon as hydrogen is introduced, the oxygen is removed and the metal particles are covered by chemisorbed hydrogen, leaving no adsorption sites for electrostatic interaction with ammonium ions. This explanation is supported by electrochemical experiments that show that NH_4^+ cannot adsorb on a clean metal surface but only adsorbs when negatively charged ions are stabilized on the electrode surface.[57]

NH₂OH₍aq₎ Adsorption. Remarkably, a hydroxylamine solution at any pH between 5 and 7 flown over either ZnSe or Al₂O₃ did not result in any observable infrared bands. In the literature, only infrared spectra of solid hydroxylamine have been reported so far.[58] The fact that no signals are observed from the solution might be due to the low extinction coefficient of dissolved hydroxylamine in water. Also, it demonstrates that no disproportionation whatsoever takes place in the absence of palladium and platinum.

When a hydroxylamine solution at pH 7 is flown over Pt/Al₂O₃, mainly adsorbed NH_4^+ (1455 cm⁻¹) was observed (Figure 5), but also nitrous oxide (2231 cm⁻¹) was observed together with an increased infrared intensity at 1570 and 1540 cm⁻¹, which will be discussed below. It has been reported that hydroxylamine undergoes a disproportionation reaction which is accelerated by the presence of metals such as platinum or palladium. In acidic media, the disproportionation results in ammonia and nitrous oxide according to the overall reaction:[42]

$$4NH_3^+OH \rightarrow 2NH_4^+ + N_2O + 2H^+ + 3H_2O \qquad (2)$$

When the spectra of Pt/Al₂O₃ and Pd/Al₂O₃ during flow of hydroxylamine at pH 5 are compared (Figure 6), clear differences can be seen. On Pd/Al₂O₃, a broad asymmetric peak was observed, which could be fitted with two bands at 1510 and 1450 cm⁻¹ (Figure 6c). The band at 1450 cm⁻¹ corresponds to the vibration of NH_4^+ (*vide ante*), indicating that at pH 5 still some disproportionation occurred on Pd/Al₂O₃, although no N₂O was detected. The observed peak at 1510 cm⁻¹ is close to what has been reported for the NH₂ scissor mode in solid NH₂OH at 1515 cm⁻¹.[58] Moreover, the NH₂ scissor mode in inorganic complexes

such as $Me(NH_2)_xCl_y$ is normally found between 1560 and 1500 cm⁻¹.[47] Further, the band is about 200 cm⁻¹ too low to be assigned to NO species on palladium.[54] For solid hydroxylamine, also a band at 1191 cm⁻¹ was reported, suggested to arise from the N—OH bending vibration in NH₂OH.[58] Further, the N—O stretch frequency in NH_3^+OH in vacuum was calculated to be at 1196 cm⁻¹.[45] In both cases, a band around 1190 cm⁻¹ is associated with the N—O bond in hydroxylamine. Clearly, in our data, this band is completely absent (Figure 6a and c), from which we conclude that the species giving rise to the peak at 1510 cm⁻¹ on Pd/Al₂O₃ is not hydroxylamine because no adsorption band was observed at 1190 cm⁻¹. As a result, we assign the band at 1510 cm⁻¹ to the scissor mode of $NH_{2(ads)}$ on palladium. Since this peak is completely stable during Ar/H₂O and O₂/H₂O flow, it can be concluded that it is strongly adsorbed on the palladium particle and cannot be easily oxidized. Recently, we showed that this species is sensitive to hydrogen and that it can be converted to ammonia.[37]

During adsorption of NH₂OH₍aq₎ at pH 5 on Pt/Al₂O₃, a peak was observed at 2231 cm⁻¹ (Figure 6a and b). This band indicates the presence of N₂O, which is dissolved in the water in the pores and voids in the catalyst layer, since it immediately disappears when Ar/H₂O is introduced (Figure 7). Nevertheless, weak adsorption on the catalyst cannot be ruled out. Since N₂O is continuously being removed from the catalyst layer by the flow of water, it must be continuously formed on Pt/Al₂O₃ in the presence of NH₂OH₍aq₎. The fact that N₂O could not be detected on palladium indicates that the rate of formation of N₂O on palladium is much lower or even absent, which is in agreement with the fact that platinum is an order of magnitude more active than palladium for the disproportionation of hydroxylamine.[42]

In addition, for Pt/Al₂O₃, a broad peak was observed centered at 1540 cm⁻¹ with a shoulder on each side. Peak fitting indicated the presence of three bands: a shoulder at 1575 cm⁻¹, a main peak at 1540 cm⁻¹, and a shoulder at 1455 cm⁻¹ (Figure 6b). The latter peak can be assigned to NH_4^+ (*vide ante*). The remarkable stability of the band at 1455 cm⁻¹ in Figure 7 indicates that the electrostatic interaction of hydrated NH_4^+ is rather strong. Apparently, the platinum surface is, at least partly, covered with O.

During subsequent Ar/H₂O flow, the band at 1540 cm⁻¹ decreased in intensity, and the peak at 1575 cm⁻¹ gained intensity and shifted gradually to 1580 cm⁻¹ after 24 min of inert flow (Figure 7), while the band at 1455 cm⁻¹ remained at its position and intensity. From Figures 6 and 7, it can be concluded that the peaks at 1540 and 1575–1580 cm⁻¹ represent two different adsorbed species. The observed blue shift for the band at 1575 cm⁻¹ with increasing intensity is characteristic for molecules with a dipole such as NO. With increasing coverage, dipole–dipole coupling occurs which causes a blue shift of the absorption band.[59,60] NO adsorbed on platinum was reported at infrared frequencies ranging from 1430 to 1800 cm⁻¹ depending on coverage, surface orientation, and experimental conditions.[12,14–19] Characterization of the water–metal interface during adsorption of NO has so far only been reported in electrochemical studies, where besides coverage and surface orientation also applied potential is influencing the infrared frequency.[16]

Table 2 summarizes the NO stretch frequencies reported on a variety of platinum surfaces in electrochemistry. Most importantly, on Pt(111) and Pt(110), bands below 1600 cm⁻¹ (bridging NO) were only observed at low NO coverage and

(57) Nightingale, R. E.; Wagner, E. L. *J. Chem. Phys.* **1954**, *22*, 203.

(59) Dunn, D. S.; Severson, M. W.; Hylden, J. L.; Overend, J. *J. Catal.* **1982**, *78*, 225–237.
(60) Hayden, B. E. *Surf. Sci.* **1983**, *131*, 419–432.

Table 2. Summary of Vibrational Frequencies for Adsorbed NO on Platinum Electrodes

| | frequency (cm^{-1}) | | | |
electrode	low coverage	high coverage	comment	ref
Pt(111)	1440	$1666 \rightarrow 1680$		16
	143	1680		12
Pt(100)	$1590 \rightarrow 1620$		shift with applied potential	14
	$1590 \rightarrow 1625$		shift with increasing coverage and applied potential	16
	between 1630 and 1610		no shift with increasing coverage	12
Pt(110)	1582	1770		15
	1590	1740		12
Pt(poly)	1580		low coverage	17,18

always detected in combination with bands above 1650 cm^{-1} (linear NO).[12,15,16] NO$_{(ads)}$ on Pt(100) only yields one peak at 1590 cm^{-1} shifting to 1625 cm^{-1} with increasing coverage and applied potential.[14-16] Finally, on polycrystalline platinum, adsorbed NO at low coverage is characterized by one single infrared frequency at 1580 cm^{-1}.[17,18]

In conclusion, the band at 1575−1580 cm^{-1} observed on Pt/Al$_2$O$_3$ in the present study can be assigned to the stretch frequency of NO$_{(ads)}$ at low coverage. Clearly, Figure 7 shows that NO$_{(ads)}$ at 1575 cm^{-1} can be produced from the species giving rise to the band at 1540 cm^{-1}, since during Ar/H$_2$O flow no hydroxylamine was present. This observation is in agreement with the literature, reporting the disproportionation of hydroxylamine in the presence of platinum either via reduction of platinum oxide by hydroxylamine or via dehydrogenation of hydroxylamine over metallic platinum, with both resulting in the formation of NO$_{(ads)}$.[42,45] Obviously, we cannot rule out that other routes to form NO$_{(ads)}$ are open when hydroxylamine is present.

This assignment is also consistent with the observation that N$_2$O forms on Pt/Al$_2$O$_3$ during NH$_2$OH$_{(aq)}$ flow, since it was shown that N$_2$O is the product of the (electro)catalytic reaction between NO and hydroxylamine on supported platinum catalysts.[42,61,62] The low coverage of NO during hydroxylamine exposure is therefore consistent with its continuous conversion into N$_2$O. Only in the absence of hydroxylamine, NO stays adsorbed on the platinum surface, and no N$_2$O is observed anymore. It was indeed published before that the rate of disproportionation of hydroxylamine increases when NO is added.[42] The presence of NO$_{(ads)}$ on Pt/Al$_2$O$_3$ and its absence on Pd/Al$_2$O$_3$ strongly suggest that the easy formation of NO from NH$_2$OH on platinum causes high activity of Pt catalysts for hydroxylamine disproportionation, as compared to the low activity of Pd/Al$_2$O$_3$ on which NO was not detected.

Finally, the only remaining band to be assigned is the peak observed on Pt/Al$_2$O$_3$ at 1540 cm^{-1}. As previously mentioned, the simultaneous decrease of the peak at 1540 cm^{-1} and increase of the 1575 cm^{-1} band in Figure 7 indicates that the species giving rise to the vibration at 1540 cm^{-1} is converted into NO$_{(ads)}$ during inert flow after hydroxylamine adsorption. According to the literature cited in Table 2, the species detected at 1540 cm^{-1} cannot be NO$_{(ads)}$ on platinum. The frequency is, on the other hand, located in the region of the scissor mode of coordinated NH$_2$ groups in inorganic complexes such as Me(NH$_2$)$_x$Cl$_y$[47,63] between 1560 and 1500 cm^{-1}. However, it is 25 cm^{-1} higher than that reported for the NH$_2$ scissor mode of solid NH$_2$OH.[58] In addition, it is 30 cm^{-1} blue-shifted compared to a similar band on palladium which was assigned above to an NH$_{2(ads)}$ species,

which would not be expected if it would be an identical adsorbate. As mentioned above, generally, adsorbed species on platinum exhibit lower vibrational frequencies compared to the same species adsorbed on palladium.[48-53] Another relevant example is the NH$_2$ scissor mode in Pt(NH$_3$)$_4$Cl$_2$ at 1563 cm^{-1}, whereas the NH$_2$ scissor mode in Pd(NH$_3$)$_4$Cl$_2$ was reported at 1601 cm^{-1}.[64] Finally, theoretical studies have shown that NH$_2$ fragments are not stable on Pt(111), which would be the most common crystal facet in our metal particles.[64] From all this, we conclude that the 1540 cm^{-1} band also cannot be due to an NH$_2$ fragment adsorbed on platinum.

Clearly, the species characterized at 1540 cm^{-1} is reactive toward oxygen (Figure 8) in contrast to NH$_{2(ads)}$ on Pd. The species is converted into a product with an absorption band at 1305 cm^{-1}. This band is identical to the peak observed during nitrite adsorption on Pt/Al$_2$O$_3$, and it was assigned to NO$_x^-$ (x = 2,3). So, it is clear that the species at 1540 cm^{-1} is formed from NH$_2$OH and still contains nitrogen. NO and NH$_2$ can be excluded based on the reasons given above. Also, H$_2$NO can be excluded, since this would give rise to an NH$_2$ scissor vibration as well as an N−O stretch frequency, but only one band is detected. The only remaining possibilities are HNO, NOH, or HNOH. It has been shown previously by theoretical calculations that HNO is the more stable fragment in vacuum.[64,65] Since the 1540 cm^{-1} species on platinum can be easily converted into NO, it is most likely HNO$_{(ads)}$ because only a single dehydrogenation step would be required. However, the other two options cannot be ruled out at this stage. Theoretical calculation of the IR absorbance of these species, taking into account the influence of the surrounding water, would be necessary to answer this question. Nevertheless, in the rest of this discussion, this species will be denoted "HNO"$_{(ads)}$.

The oxidation of "HNO"$_{(ads)}$ with O$_2$/H$_2$O results in the production of NO$_x^-{}_{(ads)}$ without a notable presence of Pt−NO, since no peak was found at 1575 cm^{-1} during oxidation. This indicates either that production of NO$_x^-{}_{(ads)}$ occurs *via* the formation of HNO$_{2(ads)}$ or that the oxidation of NO$_{(ads)}$ is much faster than the oxidation of "HNO"$_{(ads)}$.

Table 3 summarizes the assignments for the species observed in this paper. These assignments will be used in our future work on the hydrogenation of nitrate and nitrite.[37] In summary, we can conclude that Pd/Al$_2$O$_3$ and Pt/Al$_2$O$_3$ show similar adsorption behavior toward NO$_2^-{}_{(aq)}$ and NH$_4^+{}_{(aq)}$, while during the adsorption of hydroxylamine at pH 5 significant differences were observed.[37]

On Pd/Al$_2$O$_3$, hydroxylamine is converted into a stable NH$_{2(ads)}$ species, while on Pt/Al$_2$O$_3$ first "HNO"$_{(ads)}$ is observed, which decomposes into NO. These observations also explain why on

(61) Rosca, V.; Beltramo, G. L.; Koper, M. T. M. *J. Phys. Chem. B* **2004**, *108*, 8294−8304.

(62) Piela, B.; Wrona, P. K. *J. Electrochem. Soc.* **2004**, *151*, 69−79.

(63) Socrates, G. *Infrared and raman characteristic group frequencies*; John Wiley & Sons Ltd: West Sussex, U.K., 2001.

(64) Novell-Leruth, G.; Valcarcel, A.; Clotet, A.; Ricart, J. M.; Perez-Ramirez, J. *J. Phys. Chem. B* **2005**, *109*, 18061−18069.

(65) Beltramo, G. L.; Koper, M. T. M. *Langmuir* **2003**, *19*, 8907−8915.

Table 3. Peak Assignments Based on ATR-IR Data after Adsorption of NO_2^-_(aq), NH_2OH_(aq), and NH_4^+_(aq) on Pd/Al₂O₃ and Pt/Al₂O₃

infrared frequency (cm^{-1})	assignment
1235	NO_2^-_(aq)
1455	NH_4^+_(aq)
Pd/Al₂O₃	
1510	Pd-NH_2_(ads)
1450	NH_4^+_(ads) on Pd-O
1405	Pd-NO_x^-_(ads) (x = 2,3)
1325	Pd-NO_x^-_(ads) (x = 2,3)
Pt/Al₂O₃	
2231	N_2O
1575−1580	Pt-NO_(ads) (low coverage)
1540	Pt-"HNO"_(ads)
1455	NH_4^+_(ads) on Pt-O
1390	Pt-NO_x^-_(ads) (x = 2,3)
1305	Pt-NO_x^-_(ads) (x = 2,3)

Pd/Al₂O₃ no nitrous oxide is observed. Normally, N_2O is thought to be produced from either dimerization of NO, dimerization of speculated "HNO"_(ads) fragments, or a reaction between NO and adsorbed HNO.[18,20,45,66−74] Since neither NO_(ads) nor "HNO"_(ads) is observed on Pd/Al₂O₃, the formation of N_2O was not expected, which is in agreement with our experimental findings. This also agrees well with the fact that palladium is less active for the disproportionation of hydroxylamine.

Conclusion

This study convincingly shows the potential of in situ ATR-IR spectroscopy to detect and identify inorganic nitrogen compounds, that is, $NO_{2,3}^-$, NH_2, NH_4^+, NO, and HNO, adsorbed on supported metal catalysts in water.

Pd/Al₂O₃ and Pt/Al₂O₃ show similar adsorption behavior toward NO_2^-_(aq) and NH_4^+_(aq). Adsorption of NO_2^- leads to comparable adsorbed NO_x^- species on the metal particles for both catalysts, which could not be further specified. Adsorption of ammonia suggests that NH_4^+ is not chemisorbed but is interacting as hydrated ions via an electrostatic interaction on oxygen containing metal surfaces.

On the other hand, major differences were found when adsorbing NH_2OH_(aq) on Pd/Al₂O₃ and Pt/Al₂O₃. On Pd/Al₂O₃, hydroxylamine is converted into stable NH_2_(ads) fragments, which are not even reactive to oxygen, while on Pt/Al₂O₃ hydroxylamine is converted into NO via an intermediate, which is most likely HNO_(ads) or possibly NOH_(ads) or HNOH_(ads). This intermediate is reactive to oxygen, forming NO_x_(ads). These observation can explain why platinum is much more active than palladium for the disproportionation of hydroxylamine.

Supporting Information Available: Calculation of the penetration depth for ZnSe, Pt/Al₂O₃, and Pd/Al₂O₃ and the number of accessible active metal sites for Pt/Al₂O₃ and Pd/Al₂O₃. This material is available free of charge via the Internet at http://pubs.acs.org.

LA7027725

(66) Janssen, L. J. J.; Pieterse, M. M. J.; Barendrecht, E. *Electrochim. Acta* **1977**, *22*, 27−30.

(67) Paseka, I.; Vonkova, J. *Electrochim. Acta* **1980**, *25*, 1251−1253.

(68) Paseka, I.; Hodinar, A. *Electrochim. Acta* **1982**, *27*, 1461−1464.

(69) Colucci, J. A.; Foral, M. J.; Langer, S. H. *Electrochim. Acta* **1985**, *30*, 521−528.

(70) de Vooys, A. C. A.; Beltramo, G. L.; van Riet, B.; van Veen, J. A. R.; Koper, M. T. M. *Electrochim. Acta* **2004**, *49*, 1307−1314.

(71) MacNeil, J. H.; Berseth, P. A.; Westwood, G.; Trogler, W. C. *Environ. Sci. Technol.* **1998**, *32*, 876−881.

(72) Kuwabata, S.; Uezumi, S.; Tanaka, K.; Tanaka, T. *Inorg. Chem.* **1986**, *25*, 3018−3022.

(73) de Vooys, A. C. A.; Koper, M. T. M.; van Santen, R. A.; van Veen, J. A. R. *J. Catal.* **2001**, *202*, 387−394.

(74) De, D. D.; Englehardt, J. D.; Kalu, E. E. *J. Electrochem. Soc.* **2000**, *147*, 4573−4579.